This is a repository copy of *Targeted magnetic nanoparticle hyperthermia for the treatment of oral cancer*.

White Rose Research Online URL for this paper:
https://eprints.whiterose.ac.uk/149002/

Version: Accepted Version

Article:
Legge, C.J., Colley, H.E. orcid.org/0000-0003-0053-7468, Lawson, M.A. et al. (1 more author) (2019) Targeted magnetic nanoparticle hyperthermia for the treatment of oral cancer. Journal of Oral Pathology & Medicine, 48 (9). pp. 803-809. ISSN 0904-2512

https://doi.org/10.1111/jop.12921

This is the peer reviewed version of the following article: Legge, C. , Colley, H. , Lawson, M. and Rawlings, A. (2019), Targeted magnetic nanoparticle hyperthermia for the treatment of oral cancer. J Oral Pathol Med. Accepted Author Manuscript. doi:10.1111/jop.12921. This article may be used for non-commercial purposes in accordance with Wiley Terms and Conditions for Use of Self-Archived Versions.

Reuse
Items deposited in White Rose Research Online are protected by copyright, with all rights reserved unless indicated otherwise. They may be downloaded and/or printed for private study, or other acts as permitted by national copyright laws. The publisher or other rights holders may allow further reproduction and re-use of the full text version. This is indicated by the licence information on the White Rose Research Online record for the item.

Takedown
If you consider content in White Rose Research Online to be in breach of UK law, please notify us by emailing eprints@whiterose.ac.uk including the URL of the record and the reason for the withdrawal request.

eprints@whiterose.ac.uk
https://eprints.whiterose.ac.uk/

DR HELEN COLLEY (Orcid ID : 0000-0003-0053-7468)

Accepted Article

Article type : Original Article

Targeted magnetic nanoparticle hyperthermia for the treatment of oral cancer

C.J. Legge[ab], H.E. Colley[a*], M.A. Lawson[c] and A.E. Rawlings[b]

[a] School of Clinical Dentistry, University of Sheffield, 19 Claremont Crescent, Sheffield, S10 2TA, UK.

[b] Department of Chemistry, University of Sheffield, Brook Hill, S3 7HF, UK.

[c] Department of Oncology & Metabolism, University of Sheffield, Beech Hill Road, S10 2RX, UK.

*Corresponding Author:
Dr Helen Colley, School of Clinical Dentistry, University of Sheffield,
S10 2TA. Email: h.colley@sheffield.ac.uk. Tel +44(0)1142 159352

Mr Christopher Legge, Department of Chemistry, University of Sheffield, Brook Hill, S3 7HF, UK.
cjlegge1@sheffield.ac.uk

Dr Michelle Lawson, Department of Oncology & Metabolism, University of Sheffield, Beech Hill Road,
S10 2RX, UK. m.a.lawson@sheffield.ac.uk

Dr Andrea Rawlings, Department of Chemistry, University of Sheffield, Brook Hill, S3 7HF, UK.
a.rawlings@sheffield.ac.uk

This article has been accepted for publication and undergone full peer review but has not been through the copyediting, typesetting, pagination and proofreading process, which may lead to differences between this version and the Version of Record. Please cite this article as doi: 10.1111/jop.12921
This article is protected by copyright. All rights reserved.

Accepted Article

Abstract

Introduction: Patients with oral squamous cell carcinoma currently experience a five year survival rate of approximately 60% with conventional surgical, chemotherapy and radiotherapy treatments. Magnetic hyperthermia offers an alternative treatment method by utilising the heating properties of magnetic nanoparticles to produce thermo-ablation of the tumour site when exposed to an alternating magnetic field. In this study we investigate *in vitro* if targeted magnetic hyperthermia offers a potential treatment for oral squamous cell carcinoma. **Materials and methods:** Magnetic iron oxide nanoparticles, with a biocompatible silica coating, were produced and conjugated with antibodies to target integrin αvβ6, a well-characterised oral squamous cell carcinoma biomarker. Utilising the heating properties of the magnetic nanoparticles we exposed them to an alternating magnetic field to produce thermo-ablation of tumour cells either negative for or over-expressing integrin αvβ6. **Results:** The cell surface biomarker, αvβ6 integrin, was upregulated in tissue biopsies from oral squamous cell carcinoma patients compared to normal tissue. Functionalisation of the silica coating with anti-αvβ6 antibodies enabled direct targeting of the nanoparticles to αvβ6-overexpressing cells and applying thermal therapy significantly increased killing of the targeted tumour cells compared to control cells. **Conclusion:** Combining antibody-targeting magnetic nanoparticles with thermal-ablation offers a promising therapy for the targeted treatment of oral squamous cell carcinoma.

Keywords: Magnetic hyperthermia; nanoparticle; oral cancer; squamous cell carcinoma; integrin.

This article is protected by copyright. All rights reserved.

Accepted Article

Introduction:

Oral squamous cell carcinoma (OSCC) is the twelfth most common cancer worldwide, accounting for 300,000 new cases every year (1). Despite advances in conventional treatment, including surgery and radio- or chemo- therapy, the prognosis for OSCC remains poor. Survival rates have not improved over the past few decades with currently only a 60% 5 year survival rate (2). As with other cancers, there is a need to develop novel targeted methods, to not only improve efficiency but to reduce unwanted off-target side-effects that often cause considerable reduction in the quality of life for the patient.

An alternative potential cancer treatment, thermal ablation, involves applying heat (>50°C) to cause irreversible cell damage and necrosis of tumour cells (3, 4). A current challenge is delivering this heat selectively to only the site of the tumour and minimising damage of healthy tissue elsewhere. One potential solution is through the use of magnetic nanoparticles (MNP). These particles emit thermal energy when exposed to a rapidly alternating magnetic field in a process termed magnetic hyperthermia (5). This process allows the heating of cells that are closely localised to the MNP (6). In addition, the high surface area of MNP means they can be readily functionalised to enhance their biocompatibility or to immobilise drugs, or targeting agents such as antibodies. Functionalisation of the surface towards cancer cells has the potential to generate a more specific cell killing whilst simultaneously reducing off target effects on healthy tissue (7).

Cancerous cells which display unique or highly upregulated biomarkers offer the opportunity to target treatments and diagnostics to the site they are needed, and bring about a reduction in off-target side-effects (8). One such example is the heterodimeric transmembrane receptor αvβ6 integrin. This integrin is expressed on epithelial cells (9) and is highly upregulated during wound healing, as well as on the leading edge of OSCC (10, 11). The increased expression of the αvβ6 integrin in OSCC is associated with a poor prognosis and increased disease progression (12, 13). Cells

This article is protected by copyright. All rights reserved.

over-expressing the αvβ6 integrin show a more invasive phenotype, with invasion through the basement membrane and increased cell migration (14, 15). This is a direct result of αvβ6 binding to its ligand, causing the spread and development of cancer (9). The over-expression of αvβ6 integrin in tumours makes it an ideal molecule for the targeting of treatments in OSCC. By functionalising with an αvβ6 antibody, the MNP, and therefore the hyperthermia treatment, can be localised to areas of tumour growth, offering a directed therapy with the potential for significantly reduced side-effects and minimised damage to healthy tissue.

In this study we produced and characterised iron oxide MNP with a biocompatible silica shell, and conjugated them with an antibody against αvβ6. MNP were targeted specifically towards OSCC cells over-expressing αvβ6 and cell survival determined after inducing magnetic hyperthermia. We found that specific targeting of the particles increased the effectiveness of the hyperthermic treatment by increasing cell death compared to non-conjugated MNP and hyperthermic treatment alone.

Materials and Methods

All materials used were purchased from Sigma-Aldrich Company Ltd (Dorset, UK), unless otherwise stated.

Synthesis and coating of magnetic nanoparticles

Iron oxide nanoparticles were synthesised using room temperature co-precipitation with a ferric to ferrous ration of 1:1 under a nitrogen atmosphere. MNP were dispersed in ethanol. Ultrapure water and ammonium hydroxide (30%) were added to the MNP, followed by tetraethyl orthosilicate under stirring for 5 hours. The MNPs were washed and dried under vacuum. MNP were dispersed in toluene (99.9%) before addition of ammonium hydroxide (30%) and (3-aminopropyl) triethoxysilane (APTES). After stirring for 1 hour at room temperature, the MNP were washed, before drying *in vacuo*.

This article is protected by copyright. All rights reserved.

Accepted Article

Characterisation of magnetic nanoparticles

MNP were characterised using x-ray diffraction (XRD) (Bruker D8 Powder Diffractometer Bruker Corporation Billerica, Massachusetts, USA) with data collected between 20° to 80° at 0.05° intervals. MNPs diameter and shell thickness was determined using an FEI Tecnai G2 Spirit transmission electron microscope (TEM) (FEI Company, Hillsboro, Oregon, USA), with image analysis in ImageJ. MNP heating was performed in a Magnetherm alternating field generator (NanoTherics, Keele, UK) operating at a recorded field strength of 9.7 mT (Nanoscience Laboratories, Keele, UK). The coil was cooled via a recirculating water bath set at 20°C. Temperature increase during heating was recorded every 10 seconds with a fibre optic temperature probe. SAR and ILP values were calculated from the heating curve (18). A superconducting quantum interference device (SQUID) was used to measure magnetic properties at 293 K.

Antibody conjugation to the magnetic nanoparticles and ELISA.

Anti-αvβ6 mouse monoclonal antibody (clone E7P6; Merck Millipore, Darmstadt, Germany) was conjugated to the MNP using glutaraldehyde cross linking. MNP were dispersed in 2.5% glutaraldehyde solution (2 mg/ml) and sonicated for 1 hour at room temperature before washing using PBS. Anti-αvβ6 mouse mAb (10 µg/ml in PBS) was added to the glutaraldehyde-activated MNP and allowed to conjugate for 24 hours at 4°C on a roller mixer.

Conjugation of antibody was confirmed using an ELISA. The particles were blocked with Sigma Block prepared in PBS (Formedium, UK) with 0.05 % tween-20 (PBST). After one hour the MNP were supplemented with anti-mouse HRP conjugated antibody (New England Biolabs, Ipswich, Massachusetts, USA) at a ratio of 1:5000 and mixed for one hour, before transferring the MNP into fresh blocking buffer for five minutes, three times, with mixing. The particles were then magnetically collected and added to TMB reagent (Thermo Fisher, Waltham, Massachusetts, USA) for 30 minutes.

This article is protected by copyright. All rights reserved.

Accepted Article

The colour change of the supernatant at 585 nm was recorded. MNP without the conjugated anti-αvβ6 antibody were treated in the same way for comparison.

Cell culture

Two OSCC cell lines with defined integrin expression were selected; VB6 (over-expressing high levels of αvβ6) (kindly provided by Dr S Whawell) and its parent cell line H357 (negative for the αv and β6 integrin subunits), (Health Protection Agency Culture Collections, Salisbury, UK)(16) and cultured as previously described (14). Briefly, cells were cultured in flavin and adenine-enriched medium (Green's medium): Dulbecco's Modified Eagle's Medium (DMEM) and Ham's F12 medium in a 3:1 (v/v) ratio supplemented with 10% (v/v) foetal calf serum (FCS), 0.1 μM cholera toxin, 10 ng/ml epidermal growth factor, 0.4 μg/ml hydrocortisone, 0.18 mM adenine, 5 μg/ml insulin, 5 μg ml transferrin, 2 mM glutamine, 0.2 μM triiodothyronine, 0.625 μg/ml amphotericin B, 100 IU/ml penicillin and 100 μg/ml streptomycin at 37'C, 5% CO_2 (17).

Immunohistochemistry

Paraffin-embedded tissue sections (5 μm) were prepared from normal oral mucosa and archival HNSCC biopsies in accordance with the Sheffield Research Ethics Committee approval (Ref: 07/H1309/105). Sections were dewaxed, rehydrated and endogenous peroxidase neutralised with 3% hydrogen peroxide for 20 minutes. Following proteinase K antigen retrieval samples were blocked using protein-free blocking solution (Dako, Copenhagen, Denmark) for 20 minutes at room temperature and then 5 μg/ml mouse monoclonal anti-αvβ6 antibody (clone E7P6) applied for 1 hour at room temperature. Secondary antibody and avidin-biotin complex (ABC) provided with Vectastain Elite ABC kit (Vector Labs, Peterborough, UK) were then used in accordance with the manufacturer's instructions. Finally, 30-diaminobenzidine tetrahydrochloride (DAB) (VectorLabs) was used to visualise peroxidase activity and the sections were counterstained with haematoxylin, dehydrated and mounted in DPX. Images were taken using an Olympus BX51 microscope and Colour

This article is protected by copyright. All rights reserved.

Accepted Article

view IIIu camera with associated Cell^D software (Olympus Soft Imaging Solutions, GmbH, Munster, Germany).

Flow cytometry

Cells were removed from tissue culture flasks non-enzymatically, pelleted, and re-suspended in cold PBS supplemented with 1% BSA and 0.1% sodium azide (FACS buffer). Cells (1 X 10^6) were incubated with 10 µg/ml anti-αvβ6 mouse monoclonal antibody (clone 6.3G9) or IgG isotype control. Following washes with FACS buffer, cells were incubated with AlexaFlour 488-conjugated anti-mouse secondary antibody (Invitrogen, Paisley, UK) for 30 minutes on ice in the dark, then washed twice and re-suspended with FACS buffer. Flow cytometry was performed using a FACSCalibur (Becton Dickinson, San Jose, CA, USA); propidium iodide was used to gate out non-viable cells and data were analysed using FlowJo® software (FlowJo, LLC, USA).

Treatment of OSCC cells with silica magnetic nanoparticles

VB6 cells were seeded onto a 35 mm cell culture plate at a density of 1.5 X 10^5 cells and incubated for 24 hours before dosing with 0.2 mg/ml of αvβ6-MNP (αMNP) or vehicle control (uMNP). Cells were exposed to an alternating magnetic field (9.7 mT) for 10 minutes, along with appropriate controls. Cells were re-incubated for 24 and 48 hours after treatment before being analysed for cell viability using an alamarBlue® assay (Thermo Fisher, Waltham, Massachusetts, USA).

Analysis of cells after magnetic hyperthermia treatment

Cell metabolism was measured by adding alamarBlue® solution to cells (1:10 in Green's Medium) and incubating for 3 hours at 37˚C, 5 % CO_2 before removing the reagent and subjecting it to centrifugation at 1800 x *g* for 5 minutes. The alamarBlue® solution was transferred into a 96 well plate and the fluorescence measured using a spectrophotometer at a wavelength of 585 nm. After

This article is protected by copyright. All rights reserved.

Accepted Article

removal of the alamarBlue® solution, the cell plates were washed with PBS and fresh medium added before being re-incubated at 37˚C, 5 % CO_2.

Statistics

Data are presented as mean values ± standard deviation (SD) of three independent experiments (n=3), unless otherwise stated. Statistical comparisons were performed using GraphPad Prism v7.00 (GraphPad Software, La Jolla, CA, USA). Group-wise comparisons were carried out using one-way independent analysis of variance (ANOVA) with Tukey's multiple comparisons test, and differences considered significant when $p<0.05$.

Results

Production and characterisation of magnetic nanoparticles

MNP or iron oxide were synthesised using a simple room temperature coprecipitation of ferrous and ferric iron in sodium hydroxide. The solution of iron salts was added to a large excess of sodium hydroxide via a controlled dropwise addition. The resulting black precipitate was magnetically recovered, before coating with an amine terminated silica shell using conventional sol gel chemistry. The presence of surface exposed amine groups allows for convenient functionalisation later. The size and morphology of the MNP were analysed using TEM both before and after the coating step, allowing measurement of both the size of the iron oxide core and the thickness of the silica shell. The mean diameter of the uncoated MNP was found to be 8 $\pm$ 6 nm (Figure 1, A), and after coating, a uniform 6 nm thick layer of lower electron density was visible surrounding the MNP (Figure 1, B, C). The TEM images show some nanoscale clustering of particles upon drying onto the sample grid. X-ray diffraction (XRD) analysis of the MNP produced characteristic peaks consistent with the expected reflections for magnetite (ICDD card # 88-0866) (Figure 1, D), although the presence of the closely related iron oxide maghemite cannot be fully excluded. Magnetic hysteresis experiments of silica

This article is protected by copyright. All rights reserved.

Accepted Article

coated MNP revealed a coercivity of 13 Oe (Figure 1,E) and a saturation magnetisation of 56 emu/g. Due to their size and distribution it is likely that the sample comprises a mixed population of superparamagnetic and single domain ferrimagnetic particles.

We therefore exposed an 8 mg/ml aqueous suspension of the coated MNP to a rapidly alternating magnetic field (frequency of 174 kHz, magnetic field strength of 97 Oe) and recorded the heat rise of the solution using a fibre optic temperature probe. The calculated specific absorption rate (SAR) from the heating curve was 21.75 W/g with an intrinsic loss parameter (ILP) of 2.09 nHm^2/k (Figure 1, F) (18). We wanted to exploit this hyperthermic potential for OSCC cell killing and to enhance any cell killing effects by specifically targeting the particles to OSCC cells.

OSCC overexpress the integrin αvβ6

Using immunohistochemistry, we confirmed as a suitable biomarker to differentiate between normal and cancerous tissue. Patient derived normal oral mucosa and OSCC stained for αvβ6 integrin revealed expression of αvβ6 confined to the basal keratinocytes in the normal oral mucosa, but a high level of expression was present throughout the cancerous tissue (Figure 2, A-B), confirming higher expression in cancerous tissue. A panel of OSCC cell lines were screened by flow cytometry for positive expression of the αvβ6 integrin (data not shown). We selected H357 and VB6 cell lines for *in vitro* testing of our functionalised MNP experiments due to their respective negative and positive expression of the integrin (Figure 2, C).

MNP functionalisation with anti-αvβ6 antibody

The MNP were functionalised with anti-αvβ6 antibody, via glutaraldehyde crosslinking of the free amine groups of the antibody with the amine terminated surface of the silica shell. This method provides a stable, covalent linkage between the targeting molecule and the MNP. Using a modified magnetic particle-based ELISA, the antibody functionalised particles provided a positive absorbance

This article is protected by copyright. All rights reserved.

Accepted Article

reading, significantly higher compared to non-antibody conjugated controls (p=0.0009) and detection reagent alone (p=0.0024) (Figure 3), indicating successful attachment.

Anti-αvβ6-conjugated MNP targeted cytotoxity in αvβ6 overexpressing cells

Anti-αvβ6-conjugated MNP (αMNP) and unconjugated MNP (uMNP) were incubated with both the αvβ6-negative (H357) and αvβ6-positive (VB6) cell lines for 30 minutes and exposed to an alternating magnetic field (AMF) for a single 10 minute treatment to induce magnetic hyperthermia (MHT). Cell survival was measured at 24 and 48 hours post treatment using an alamarBlue® assay (Figure 4). After 24 hours no effect on cell death was seen in the H357 cells treated with either αMNP or uMNP in both the hyperthermia or no hyperthermia groups (Figure 4, A-B). At 48 there is a small effect on both the viability of αMNP and uMNP treatment groups that underwent hyperthermia but there is no significant difference between the targeted and untargeted treatment groups (Figure 4, C-D). In contrast the Vβ6 cell lines showed increased susceptibility to the presence of both αMNP or uMNP without hyperthermia compared with the H357 cell line but in the αMNP targeted population undergoing hyperthermia there was a greater, more significant, decrease to below 50% of the control at 24 hours and below 25 % at 48 hours.

Discussion

More effective treatments against OSCC are urgently needed to improve outcomes and survival rates for patients. We have therefore, for the first time, brought together the emerging field of magnetic hyperthermia for cell heating and destruction, with an under exploited biomarker for OSCC, resulting in a promising new targeted treatment approach.

Iron oxide nanoparticles have been the subject of many studies into their use as magnetic hyperthermia agents, due to their intrinsic magnetic properties and biocompatibility (19). In particular, the iron oxide magnetite has favourable magnetic properties for hyperthermia treatment, but this is dependent on the size and shape of the particles used. We wanted to produce magnetite

This article is protected by copyright. All rights reserved.

Accepted Article

nanoparticles with suitable characteristics to allow them to be readily taken up into cells, and, crucially, still possess sufficient heating potential for cell killing. Previous studies which have investigated cellular uptake of iron oxide nanoparticles, suggest that the smaller the particles the higher the level of uptake (19) . This clearly needs to be balanced against the heating potential, whereby larger particles generally display greater levels of magnetically induced heating (20). To this end, we employed a synthesis of magnetite using a simple room temperature co-precipitation of Fe^{2+}/Fe^{3+} ions. The TEM particle sizing, powder XRD pattern, and coercivity are all consistent with small 8-12 nm magnetite nanoparticles. The measured SAR value matches that observed for similarly sized magnetite nanoparticles which achieve hyperthermia via Néel and Brownian modes (5).

We encapsulated the particles within an amine terminated silica shell in order to preserve the magnetite core from oxidation, minimise any unwanted cytotoxicity, and provide a functionalised surface for convenient conjugation to antibodies (21). In addition, silica coating has previously been shown to improve cellular uptake of iron oxide nanoparticles (22).

In agreement with others, the αvβ6 integrin is highly expressed by OSCC tumour cells, making it a suitable target molecule for antibody-directed therapy (23). Being able to specifically target such MNP to cancer cells, allows for efficient heating and destruction of tumour cells whilst minimising effects on healthy tissue. We have demonstrated this *in vitro*, where MNP displaying an anti-αvβ6 antibody resulted in the death of 85% of VB6 cells with only a single 10 minute exposure to an alternating magnetic field. This is in contrast to only a 20% reduction in cell viability for αvβ6-negative (H357) cells exposed to the same regime. A further reduction in cell viability, for cultures exposed to both MNP and the alternating magnetic field, in both cell lines 48 hours after treatment compared to 24 hours was also observed. The addition of αMNP to both cell lines reveals a significant reduction in cell viability in VB6 experiments, both at 24 and 48 hours post addition, with negligible effects observed in the H357 cells which display lower levels of the target biomarker. This suggests that the presence of the antibody modulates MNP interaction with the cells, and negatively

This article is protected by copyright. All rights reserved.

Accepted Article

impacts cells over expressing the αvβ6 receptor. Once coupled with MHT the VB6 cells show decreased cell survival with the αMNP compared with uMNP at both 24 and 48 hours post MHT treatment. In comparison, H357 cells exposed to the same regime showed no difference in effectiveness between the uMNP and αMNP. Only VB6 cells, treated with the αVβ6 antibody-targeted therapy, produced a significant drop in cell viability at both 24 ($p<0.0001$) and 48 ($p<0.0001$) hours. Interestingly the cell survival in αMNP treated VB6 cells continues to fall between 24 and 48 hours after MHT. We surmise that the cells may have undergone their first complete cell cycle during the 24 to 48-hour time points post MHT, which suggests that apoptosis may be occurring as the cells undergo division, perhaps triggered by cellular damage that is not immediately lethal. A similar effect is observed in H357 cells where MHT exposed cells also show a decrease in survival between 24 and 48 hours post treatment. At 48 hours post treatment, both cell lines exposed to uMNP and MHT, as well as the αMNP in the H357 experiment, produced very similar levels of cell viability. In these cases, we would anticipate that the MNP are behaving in an untargeted fashion and represent the background level of cell killing produced from non-specific, residual levels of MNP when MHT is applied. This also confirms that the presence of both the antibody and over expressed receptor are required in order to access higher levels of cell killing.

In summary, we have synthesised and tested a MHT agent which is targeted towards VB6 cells associated with OSCC. Our results indicate efficient and significant cell killing when exposed to an alternating magnetic field, and only when the VB6 antibody is adequately paired with its cognate antigen. This promising *in vitro* study indicates that through careful pairing of antigen, antibody and nanoparticle, the killing potential of OSCC by magnetic hyperthemia can be significantly enhanced.

This article is protected by copyright. All rights reserved.

Accepted Article

Accepted Article

Acknowledgments

The authors thank Dr Sarah Staniland for the use of her laboratory and equipment and Professor Craig Murdoch for critical review of the manuscript. We would also like to thank the Sheffield Electron Microscopy Unit for TEM assistance, Sharon Spey for powder X-ray diffraction data collection and Aliaa Zaki for assistance with SQUID measurement.

Conflicts of Interest

The authors have no conflicts of interest to disclose.

References

1. Bray F, Ferlay J, Soerjomataram I, Siegel RL, Torre LA, Jemal A. Global cancer statistics 2018: GLOBOCAN estimates of incidence and mortality worldwide for 36 cancers in 185 countries. Ca-a Cancer Journal for Clinicians. 2018;68(6):394-424.
2. Pulte D, Brenner H. Changes in Survival in Head and Neck Cancers in the Late 20th and Early 21st Century: A Period Analysis. Oncologist. 2010;15(9):994-1001.
3. Haen SP, Pereira PL, Salih HR, Rammensee HG, Gouttefangeas C. More Than Just Tumor Destruction: Immunomodulation by Thermal Ablation of Cancer. Clin Dev Immunol. 2011:19.
4. Zhao Q, Wang L, Cheng R, Mao L, Arnold RD, Howerth EW, et al. Magnetic nanoparticle-based hyperthermia for head & neck cancer in mouse models. Theranostics. 2012;2:113-21.
5. Obaidat IM, Issa B, Haik Y. Magnetic Properties of Magnetic Nanoparticles for Efficient Hyperthermia. Nanomaterials (Basel). 2015;5(1):63-89.
6. Rivas J, Banobre-Lopez M, Pineiro-Redondo Y, Rivas B, Lopez-Quintela MA. Magnetic nanoparticles for application in cancer therapy. Journal of Magnetism and Magnetic Materials. 2012;324(21):3499-502.
7. Banobre-López M, Teijeiro A, Rivas J. Magnetic nanoparticle-based hyperthermia for cancer treatment. Reports of practical oncology and radiotherapy; 2013. p. 397–400.
8. Parekh P, Kamble S, Zhao NX, Portier BP, Zu YL. Immunotherapy of CD30-expressing lymphoma using a highly stable ssDNA aptamer. Biomaterials. 2013;34(35):8909-17.
9. Bandyopadhyay A, Raghavan S. Defining the Role of Integrin αvβ6 in Cancer. Curr Drug Targets; 2009. p. 645–52.
10. Xue H, Atakilit A, Zhu WM, Li XW, Ramos DM, Pytela R. Role of the alpha v beta 6 integrin in human oral squamous cell carcinoma growth in vivo and in vitro. Biochem Biophys Res Commun. 2001;288(3):610-8.
11. Ylipalosaari M, Thomas GJ, Nystrom M, Salhimi S, Marshall JF, Huotari V, et al. alpha v beta 6 integrin down-regulates the MMP-13 expression in oral squamous cell carcinoma cells. Exp Cell Res. 2005;309(2):273-83.
12. Regezi JA, Ramos DM, Pytela R, Dekker NP, Jordan RCK. Tenascin and beta 6 integrin are overexpressed in floor of mouth in situ carcinomas and invasive squamous cell carcinomas. Oral Oncology. 2002;38(4):332-6.

This article is protected by copyright. All rights reserved.

13. Hamidi S, Salo T, Kainulainen T, Epstein J, Lerner K, Larjava H. Expression of alpha(v)beta(6) integrin in oral leukoplakia. British Journal of Cancer. 2000;82(8):1433-40.
14. Thomas GJ, Lewis MP, Whawell SA, Russell A, Sheppard D, Hart IR, et al. Expression of the alpha v beta 6 integrin promotes migration and invasion in squamous carcinoma cells. Journal of Investigative Dermatology. 2001;117(1):67-73.
15. Ramos D, Dang D, Sadler S. The Role of the Integrin αvβ6 in Regulating the Epithelial to Mesenchymal Transition in Oral Cancer. Anticancer Res; 2002. p. 125-30.
16. Prime SS, Nixon SVR, Crane IJ, Stone A, Matthews JB, Maitland NJ, et al. THE BEHAVIOR OF HUMAN ORAL SQUAMOUS-CELL CARCINOMA IN CELL-CULTURE. Journal of Pathology. 1990;160(3):259-69.
17. Allenhoffmann BL, Rheinwald JG. POLYCYCLIC AROMATIC HYDROCARBON MUTAGENESIS OF HUMAN EPIDERMAL-KERATINOCYTES IN CULTURE. Proceedings of the National Academy of Sciences of the United States of America-Biological Sciences. 1984;81(24):7802-6.
18. Wildeboer RR, Southern P, Pankhurst QA. On the reliable measurement of specific absorption rates and intrinsic loss parameters in magnetic hyperthermia materials. Journal of Physics D-Applied Physics. 2014;47(49):14.
19. Feng QY, Liu YP, Huang J, Chen K, Huang JX, Xiao K. Uptake, distribution, clearance, and toxicity of iron oxide nanoparticles with different sizes and coatings. Scientific Reports. 2018;8:13.
20. Nemati Z, Alonso J, Rodrigo I, Das R, Garaio E, Garcia JA, et al. Improving the Heating Efficiency of Iron Oxide Nanoparticles by Tuning Their Shape and Size. Journal of Physical Chemistry C. 2018;122(4):2367-81.
21. catalano E, Miola M, Ferraris S, Novak S, Francesca O, Cochis A, et al. Magnetite and silica-coated magnetite nanoparticles are highly biocompatible on endothelial cells in vitro. Biomedical Physics & Engineering Express; 2017.
22. Malvindi MA, De Matteis V, Galeone A, Brunetti V, Anyfantis GC, Athanassiou A, et al. Toxicity Assessment of Silica Coated Iron Oxide Nanoparticles and Biocompatibility Improvement by Surface Engineering. Plos One. 2014;9(1):11.
23. Bandyopadhyay A, Raghavan S. Defining the Role of Integrin alpha v beta 6 in Cancer. Current Drug Targets. 2009;10(7):645-52.

Accepted Article

This article is protected by copyright. All rights reserved.

Accepted Article

Figure Legends

Figure 1: Magnetic nanoparticle characterisation. (A) TEM images of synthesised MNP and (B) silica coated MNP. (C) Frequency distribution of MNP. (D) XRD of MNP with peaks corresponding to the iron oxide magnetite. (E) SQUID magnetic hysteresis measurements of coated MNP. (F) Temperature increase of MNP when exposed to an alternating magnetic field. Scale bar = 40 nm.

Figure 2: Biomarker selection. Immunohistochemical analysis of (A) normal and (B) OSCC reveal that αvβ6 integrin is expressed exclusively on basal keratinocytes in normal tissue whilst expression is observed in all epithelial cells in OSCC. (C) Flow cytometry analysis of the αvβ6 integrin expression on H357 and the overexpressing VB6 cell line demonstrates that H357 are negative for the integrin whilst VB6 show a positive expression on 65% of the cell population (n=3). Scale bar = 50 μm.

Figure 3: Antibody conjugation. An enzyme-linked immunosorbent assay comparing MNP before and after anti-αvβ6 integrin conjugation revealed antibody stably bound to the surface of the MNP (n=3). **denotes a statistically significant difference of $p<0.01$ and *** $p<0.001$.

Figure 4: Targeted magnetic nanoparticle hyperthermia treatment. H357 and VB6 cell monolayers were exposed to either anti-αvβ6 conjugated MNP, un-conjugated MNP or no particles for 1 hour before exposure to an alternating magnetic field for 10 minutes. Cells were cultured for a further 24 and 48 hours and cell survival measured using alamarBlue® (n=3). **denotes a statistically significant difference of $p<0.01$, *** $p<0.001$ and **** $p<0.0001$.

This article is protected by copyright. All rights reserved.

Accepted Article

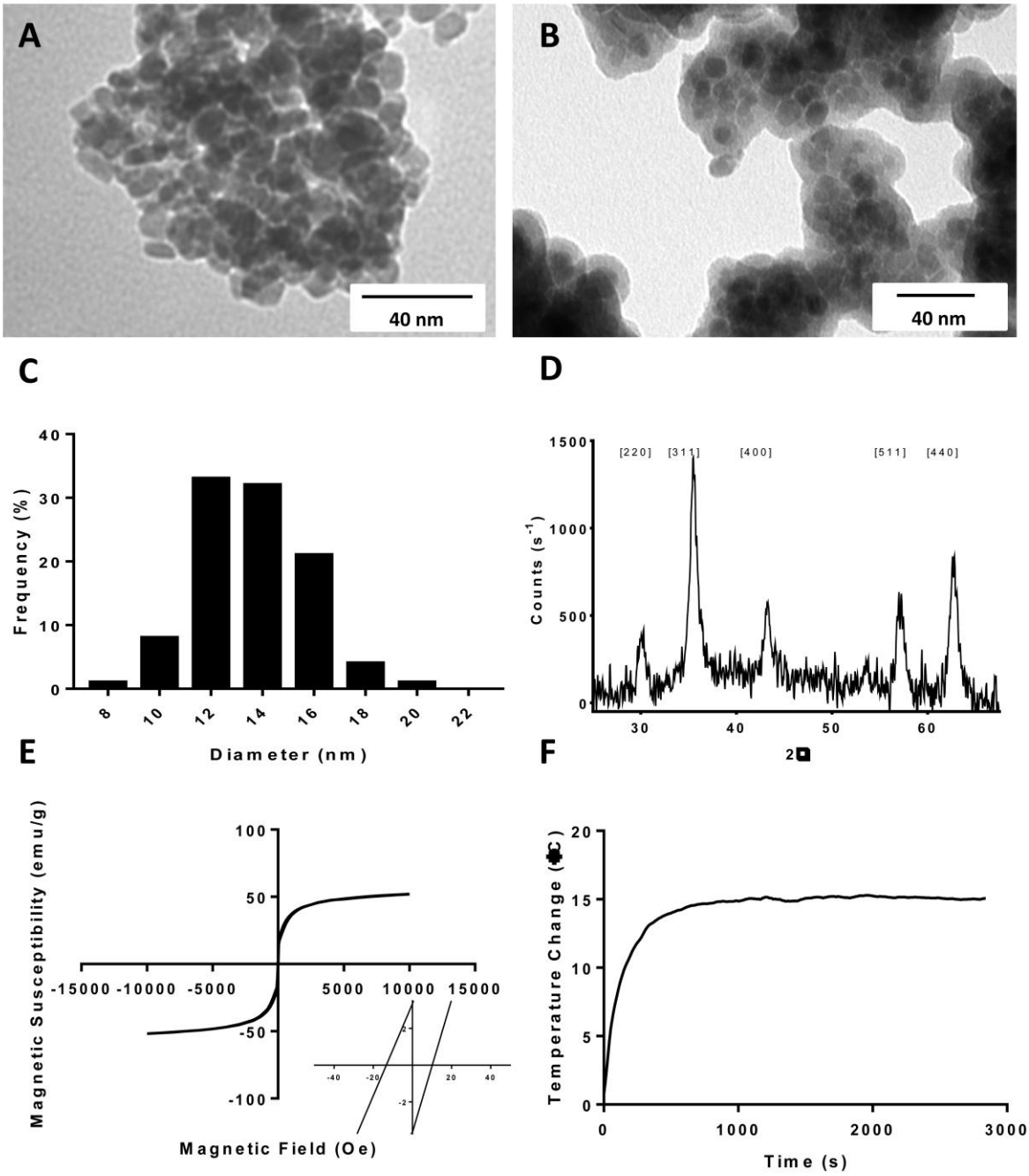

This article is protected by copyright. All rights reserved.

Accepted Article

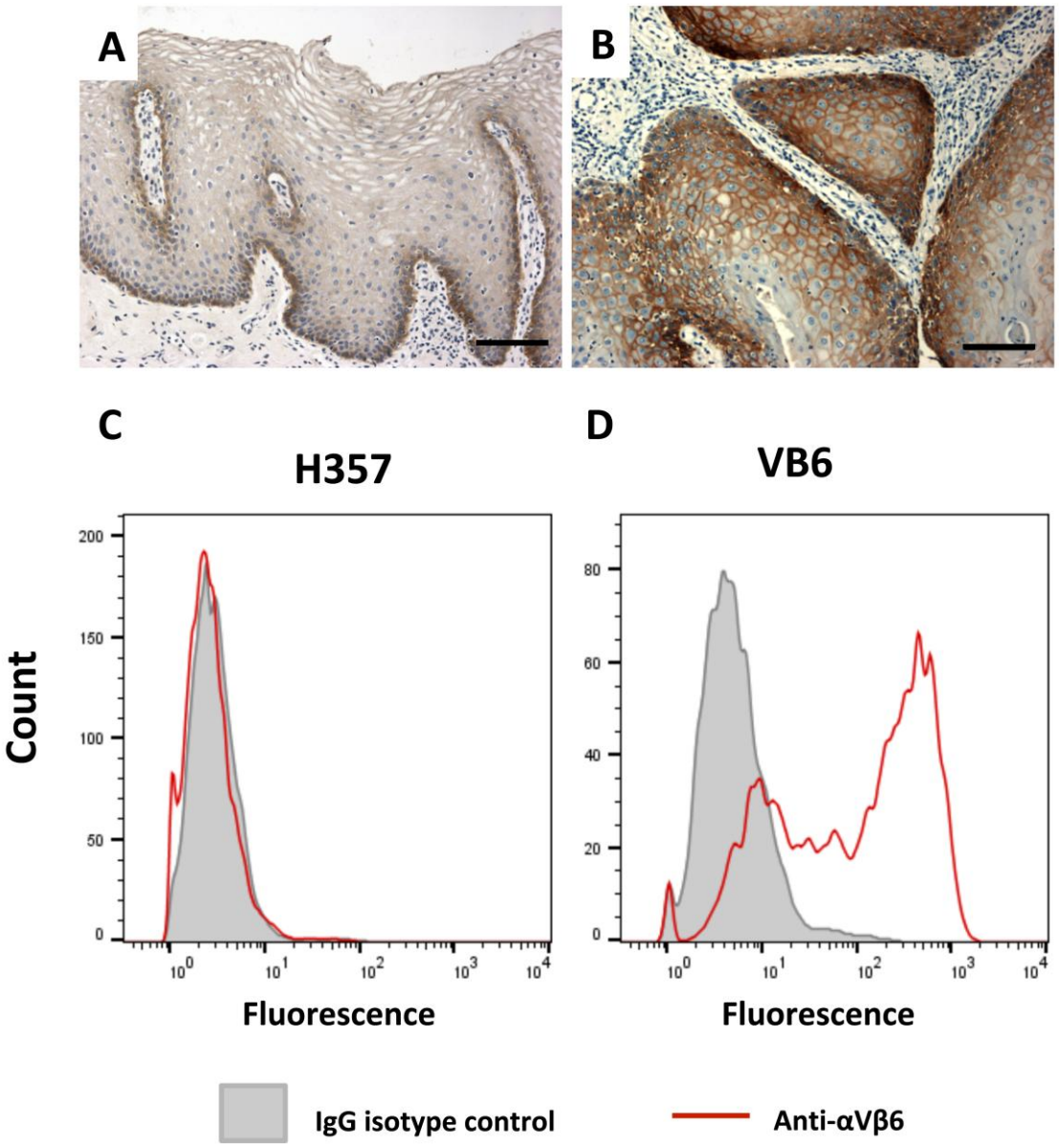

This article is protected by copyright. All rights reserved.

Accepted Article

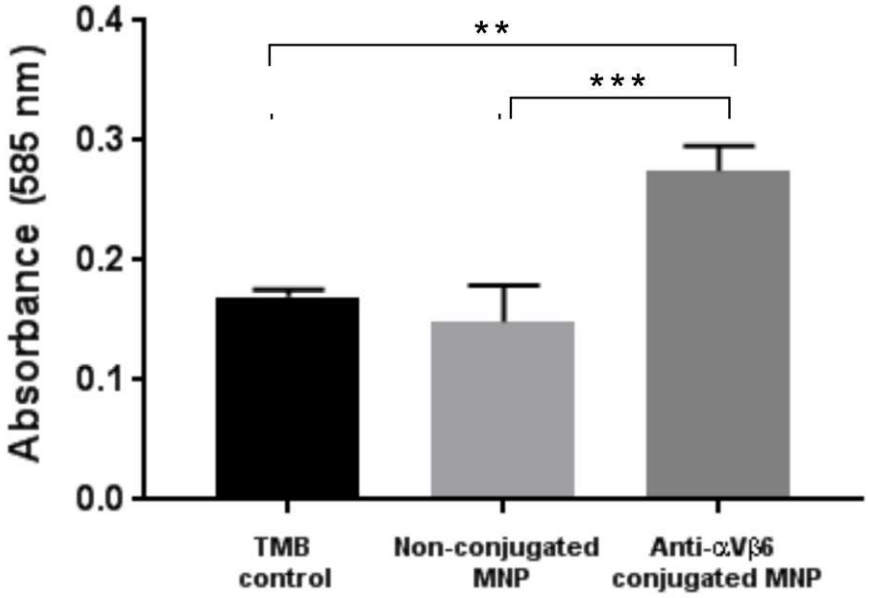

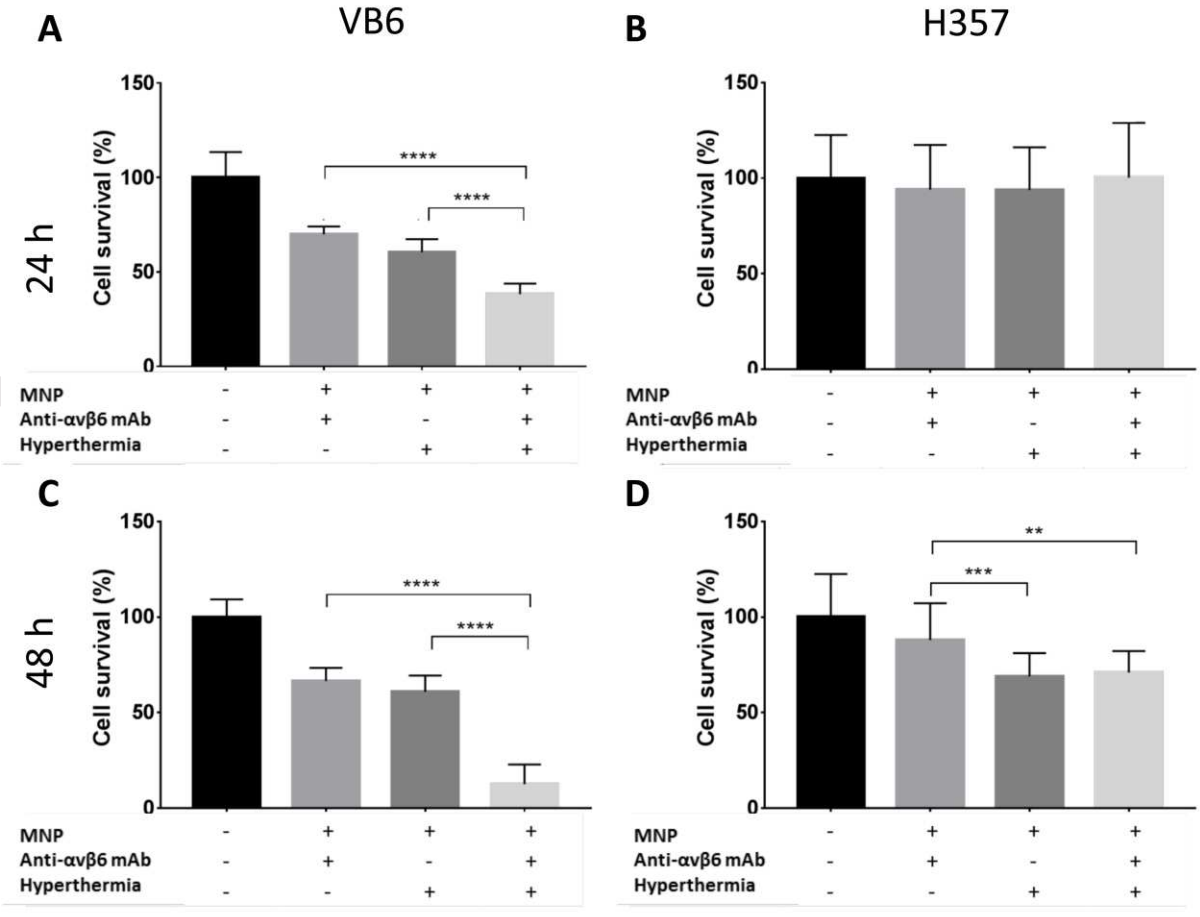

This article is protected by copyright. All rights reserved.